Charge Storage Mechanism of MnO_2 Electrode Used in Aqueous Electrochemical Capacitor

Mathieu Toupin,[†] Thierry Brousse,*[,†,‡] and Daniel Bélanger*[,†]

Département de Chimie, Université du Québec à Montréal, Case Postale 8888, succursale Centre-Ville, Montréal, Québec H3C 3P8, Canada, and Laboratoire de Génie des Matériaux, Ecole Polytechnique de l'Université de Nantes, La Chantrerie, rue Christian Pauc, BP50609, 44306 Nantes Cedex 3, France

Received March 2, 2004. Revised Manuscript Received June 2, 2004

The charge storage mechanism in MnO_2 electrode, used in aqueous electrolyte, was investigated by cyclic voltammetry and X-ray photoelectron spectroscopy. Thin MnO_2 films deposited on a platinum substrate and thick MnO_2 composite electrodes were used. First, the cyclic voltammetry data established that only a thin layer of MnO_2 is involved in the redox process and electrochemically active. Second, the X-ray photoelectron spectroscopy data revealed that the manganese oxidation state was varying from III to IV for the reduced and oxidized forms of thin film electrodes, respectively, during the charge/discharge process. The X-ray photoelectron spectroscopy data also show that Na^+ cations from the electrolyte were involved in the charge storage process of MnO_2 thin film electrodes. However, the Na/Mn ratio for the reduced electrode was much lower than what was anticipated for charge compensation dominated by Na^+, thus suggesting the involvement of protons in the pseudofaradaic mechanism. An important finding of this work is that, unlike thin film electrodes, no change of the manganese oxidation state was detected for a thicker composite electrode because only a very thin layer is involved in the charge storage process.

Introduction

Electrochemical supercapacitors are currently investigated in various academic and industrial laboratories because they can be used as complementary charge storage devices to conventional batteries in various applications that require peak power pulses.[1,2] In these electrochemical supercapacitors, the energy being stored is either capacitive or pseudocapacitive in nature. The capacitive or nonfaradaic process is based on charge separation at the electrode/solution interface, whereas the pseudocapacitive process consists of faradaic redox reactions that occur within the active electrode materials. The most widely used active electrode materials are carbon,[3,4] conducting polymers,[5,6] and both noble[7−9] and transition-metal oxides.[10−29]

The main motivation for the use of transition-metal oxides lies in their low cost compared to noble metal oxides such as ruthenium[7,8] and iridium[9] oxides. The initial studies were performed on nickel oxide[10] and cobalt oxide[11] but more recently iron[12−15] and manganese oxides[14,16−29] were investigated. The research efforts focused on compounds providing high cyclability and capacitance. On the other hand, the charge storage mechanism of MnO_2 has not been investigated in detail. Until now, two mechanisms were proposed to explain the MnO_2 charge storage behavior. The first one implies the intercalation of protons (H^+) or alkali metal cations (C^+) such as Li^+ in the bulk of the material upon reduction followed by deintercalation upon oxidation.[17]

$$MnO_2 + H^+ + e^- \leftrightarrow MnOOH \quad (1)$$

or

$$MnO_2 + C^+ + e^- \leftrightarrow MnOOC \quad (2)$$

The second mechanism is based on the surface adsorption of electrolyte cations (C^+) on MnO_2[16]

$$(MnO_2)_{surface} + C^+ + e^- \leftrightarrow (MnO_2{}^-C^+)_{surface} \quad (3)$$

where $C^+ = Na^+, K^+, Li^+$. This mechanism was proposed following the observation of significant difference of the cyclic voltammogram and the capacitance of MnO_2 in the presence of various metal alkali cations in the electrolyte.[16] It should be noticed that both proposed

* To whom correspondence should be addressed. E-mail: thierry.brousse@polytech.univ-nantes.fr (T.B.) and belanger.daniel@uqam.ca (D.B.).
[†] Université du Québec à Montréal.
[‡] Ecole Polytechnique de l'Université de Nantes.

(1) Conway, B. E. *Electrochemical Supercapacitors, Scientific Fundamentals and Technological applications*; Kluwer Academic/Plenum Press: New York, 1999.
(2) Burke, A. *J. Power Sources* **2000**, *91*, 37.
(3) Frackowiak, E.; Béguin, F. *Carbon* **2001**, *39*, 937.
(4) Lin, C.; Popov, B. N.; Ploehn, H. J. *J. Electrochem. Soc.* **2002**, *149*, A167.
(5) Villers, D.; Jobin, D.; Soucy, C.; Cossement, D.; Chahine, R.; Breau, L.; Bélanger, D. *J. Electrochem. Soc.* **2003**, *150*, A747.
(6) Fusalba, F.; El Mehdi, N.; Breau, L.; Bélanger, D. *Chem. Mater.* **2000**, *12*, 2581.
(7) Zheng, J. P.; Jow, T. R. *J. Electrochem. Soc.* **1995**, *142*, L6.
(8) Soudan, P.; Gaudet, J.; Guay, D.; Bélanger, D.; Schulz, R. *Chem. Mater.* **2002**, *14*, 1210.
(9) Conway, B. E.; Birss, V.; Wojtowicz, J. *J. Power Sources* **1997**, *66*, 1.
(10) Nelson, P. A.; Owen, J. R. *J. Electrochem. Soc.* **2003**, *150*, A1313.

10.1021/cm049649j CCC: $27.50
Published on Web 07/16/2004

mechanisms involved a redox reaction between the III and IV oxidation states of Mn.

The mechanism based on the solid-state diffusion of protons in the bulk of the material is similar to that proposed for RuO_2.[7] However, only a limited fraction of the MnO_2 composite is electrochemically active, thus suggesting that the protonic diffusion in the bulk of the MnO_2 compound might not be as fast as in the case of RuO_2.[21] Subsequently, the charge storage might only involved the surface atoms of the MnO_2 crystallites or a very thin layer. Then it might be plausible to assume that ions from the electrolyte would participate in the charge compensation process. On the other hand, the reported capacitance ranging between 150 and 200 F/g for composite electrode cannot be only associated to the formation of the classical double layer.[21] Hence, the nature of the charge storage mechanism must be pseudocapacitive.

This work aimed at getting a better understanding of the charge storage mechanism in manganese dioxide electrodes when cycled in aqueous electrolyte. The electrodes were characterized by cyclic voltammetry and X-ray photoelectron spectroscopy in order to determine a change of the manganese valence upon charge/discharge. Additionally, the experimental results were used to determine whether the charge storage process was limited to the surface of the oxide or if it occurred inside the bulk of the material.

Experimental Section

Preparation of the MnO_2 Powder. The MnO_2 powder was synthesized by coprecipitation.[21] Briefly, $KMnO_4$ and $MnSO_4 \cdot H_2O$ were mixed in a 2:3 molar ratio, leading to a dark brown precipitate. The amorphous nature of the as-synthesized MnO_2 powder was confirmed by the X-ray diffraction (XRD) spectrum (Figure SI1), which shows broad peaks related to a poorly crystallized compound. From chemical analysis, the stoichiometry for the powder was determined to be $K_{0.02}MnO_2H_{0.33}$, $0.53H_2O$. Thereafter, the compound will be named "MnO_2" despite that it does not reflect the exact composition of the sample.

Scanning electron micrographs revealed that the as-synthesized α-MnO_2 powder is made of spherical grains (Figure SI2). The length scale is systematically indicated as a white bar on the bottom left corner of the micrographs. A statistical analysis of the grain diameter performed over more than 100 particles yielded a Gaussian distribution centered at 420 nm with a standard deviation of 190 nm. Each grain seems to result from the agglomeration of smaller particles (Figure SI3). Using the geometric surface of spherical grains (420 nm diameter assuming a density of 4.8 g/cm^3) the specific surface was estimated to a value close to 3 m^2/g. The specific surface area determined from BET measurements (160 $\pm$ 3 m^2/g) is larger than this value thus indicating that pores and voids exist inside the grains examined by scanning electron microscopy.

Preparation of the Electrodes. To investigate the influence of both the thickness and the composition of the electrodes, thick film ($\approx$100 μm) and thin film ($<$5 μm) electrodes were prepared. For the thick film samples, a composite was typically prepared by mixing 80% of active powder, 7.5% of graphite (Alfa Aesar), 7.5% of acetylene black (Alfa Aesar), and 5% of PTFE (poly(tetrafluoroethylene), Dupont) in ethanol (Fisher). Then, cold rolling of the obtained paste resulted in a black shiny film, which was pressed in a ply of a stainless steel mesh (Alfa Aesar, 200 mesh) current collector under a pressure of 9 metric tons (see Figure SI4a for a photomicrograph of these electrodes). Typically, a 2 mg square piece of film was used for the electrode, referred to as "composite" electrodes from now on.

Alternatively, thin films were prepared by dispersing an appropriate amount of MnO_2 in a solution of polyvinylidene difluoride-hexafluoropropylene (copolymer PVdF−HFP, Kynarflex) in *N*-methyl pyrolydinone (NMP, Fisher) to obtain a final concentration of 1 mg (MnO_2)/mL with 10% w/w of polymer. The dispersion was left in a ultrasonic bath for 30 min. A platinum foil (1.5 $\times$ 0.5 cm; thickness 0.1 mm; Alfa Aesar) was used as the substrate (and current collector) and coated with the MnO_2 slurry by adding 5 μL drops of the dispersion with a micropipet (Eppendorf) (see Figure SI4b for a photomicrograph of these electrodes). The electrode was dried in a oven at 65 °C for 30 min between each drop. Typically the area of platinum covered with the slurry was 0.75 cm $\times$ 0.5 cm. The mass of the deposited material was deduced by weighing the electrode before and after the coating. Thereafter, these electrodes will be referred to as "thin film" electrodes. However, this denomination is not totally correct since the "film" is most likely seen as aggregates of MnO_2 particles (thickness is less than 2 μm) on the platinum substrate (see Figure SI4b).

Electrochemical Measurements. The cyclic voltammetry and polarization experiments were carried out with a 1470 multipotentiostat (Solartron, Mobrey) using the Corrware software (Scribner Associates, version 2.6). A beaker type cell containing a 0.1 M Na_2SO_4 electrolyte solution was used for all the electrochemical measurements. The cyclic voltammetry experiments were performed between 0 and 0.9 V vs Ag/AgCl (3 M NaCl) at a scan rate of 5 mV/s.

The specific capacitance, C_{cv}, was calculated using the voltammetric charge integrated from the cyclic voltammogram according to the following equation

$$C_{cv} = \frac{Q}{\Delta E \times m} \tag{4}$$

where C_{cv} is the specific capacitance (in F/g), Q is the charge (in C), ΔE is the potential window (in V), and m is the mass of active material (in g).

Surface Characterization of the Electrodes. After polarization, the electrodes were dried out in a vacuum oven at ambient temperature for 1 hour. The XPS studies were conducted with a VG Escalab 220i-XL instrument equipped with a hemispherical analyzer and using an aluminum anode (monochromatic K_α X-rays at 1486.6 eV) as a source (at 12−14 kV and 10−20 mA). The XPS spectra were analyzed and fitted using CasaXPS software (version 2.2.27). The C 1s region

(11) Lin, C.; Ritter, J. A.; Popov, B. N. *J. Electrochem. Soc.* **1998**, *145*, 4097.
(12) Wu, N.-L.; Wang, S.-Y.; Han, C.-Y.; Wu, D.-S.; Shiue, L.-R. *J. Power Sources* **2003**, 113, 173.
(13) Wu, N. L. *Mater. Chem. Phys.* **2002**, *75*, 6.
(14) Brousse, T.; Bélanger, D. *Electrochem. Solid-State Lett.* **2003**, *6*, A244.
(15) Brousse, T.; Delahaye, T.; Bélanger, D. In preparation.
(16) Lee, H. Y.; Goodenough, J. B. *J. Solid State Chem.* **1999**, *144*, 220. See also a more detailed version of this study in the following: Lee, H. Y.; Manivannan, V.; Goodenough, J. B. C. R. *Acad. Sci. Paris* **1999**, *t. 2, Série II c*, 565.
(17) Pang, S. C.; Anderson, M. A.; Chapman, T. W. *J. Electrochem. Soc.* **2000**, *147*, 444.
(18) Lee, H. Y.; Kim, S. W.; Lee, H. Y. *Electrochem. Solid-State Lett.* **2001**, *4*, A19.
(19) Hu, C. C.; Tsou, T. W. *Electrochem. Comm.* **2002**, *4*, 105.
(20) Chin, S. F.; Pang, S. C.; Anderson, M. A. *J. Electrochem. Soc.* **2002**, *149*, A379.
(21) Toupin, M.; Brousse, T.; Bélanger, D. *Chem. Mater.* **2002**, *14*, 3946.
(22) Brousse, T.; Toupin, M.; Bélanger, D. *J. Electrochem. Soc.* **2004**, *151*, A614.
(23) Jiang, J.; Kucernak, A. *Electrochim. Acta* **2002**, *47*, 2381.
(24) Hu, C. C.; Tsou, T. W. *Electrochim. Acta* **2002**, *47*, 3523.
(25) Jeong, Y. U.; Manthiram, A. *J. Electrochem. Soc.* **2002**, *149*, A1419.
(26) Broughton, J. N.; Brett, M. J. *Electrochem. Solid-State Lett.* **2002**, *5*, A279.
(27) Kim, H.; Popov, B. N. *J. Electrochem. Soc.* **2003**, *150*, D56.
(28) Hu, C.-C.; Wang, C.-C. *J. Electrochem. Soc.* **2003**, *150*, A1079.
(29) Chang, J.-K.; Tsai, W.-T. *J. Electrochem. Soc.* **2003**, *150*, A1333.

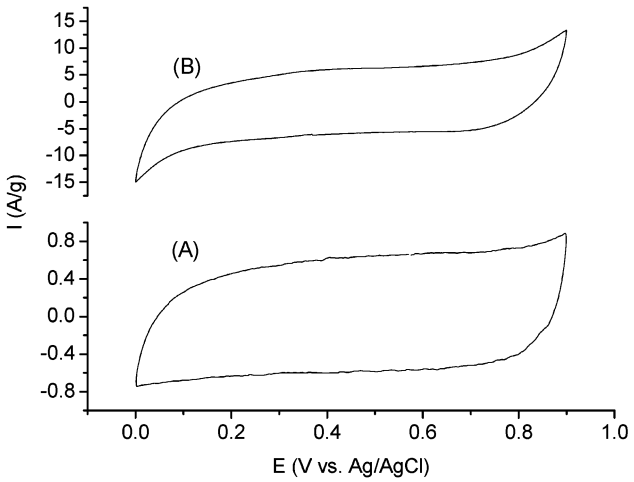

Figure 1. Cyclic voltamograms in 0.1 M Na_2SO_4 at 5 mV/s of (A) a composite electrode composed of 80% MnO_2, 7.5% graphite, 7.5% acetylene black, and 5% Teflon and (B) a 90% MnO_2 and 10% PVdF−HFP thin film electrode supported on a Pt foil.

was used as a reference for surface charging and was set at 284.9 eV. A mixture of Gaussian (70%) and Lorentzian (30%) functions was used for the least-squares curve fitting procedure.

The manganese oxidation state was determined from the Mn 3s and O 1s core level spectra. The procedure used to analyze the Mn 3s spectra has been described previously.[21,30,31] In the case of the O 1s data, the average manganese oxidation state for the three electrodes can be computed from the intensities of the Mn−O−Mn and Mn−OH components according to

$$\text{Ox·State} = \frac{(\text{IV}^*(S_{\text{Mn-O-Mn}} - S_{\text{Mn-OH}})) + (\text{III}^*S_{\text{Mn-OH}})}{S_{\text{Mn-O-Mn}}} \quad (5)$$

where S stands for signal of the different components of the O 1s spectra. Since all manganese atoms are bonded to an oxygen atom, the Mn−O−Mn signal should represent the contribution of two species: MnOOH and MnO_2. Hence, the XPS signal related to the Mn(IV) species can be computed by subtracting the contribution of the hydroxyl group (Mn−OH) from the Mn−O−Mn signal. Binding energies and manganese oxidation states of authentic samples can be found in Table 1 of ref 30.

Results and Discussion

Electrochemical Behavior of the MnO_2 Composite Electrode. Figure 1A shows a typical cyclic voltammogram for a composite film electrode in 0.1 M Na_2SO_4 at a scan rate of 5 mV/s. The cyclic voltammetry response when the negative and positive potential limits are restricted to 0 and 0.9 V, respectively, is characteristic of a pseudocapacitive electrode material, but it is not perfectly rectangular due to polarization resistance. This effect is noticeably more significant at the less positive potential limit compared to the positive limit, and this specific point will be discussed later. The cyclic voltammogram is similar to that previously reported for MnO_2-based composite electrode, and a capacitance of 150 F/g can be computed for this electrode.[14,21,22]

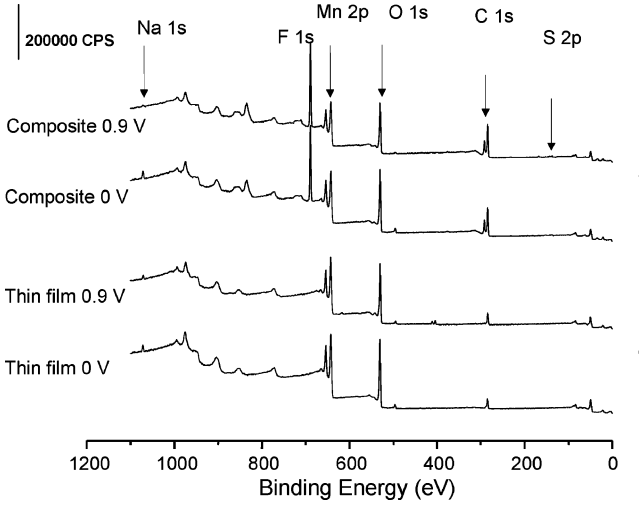

Figure 2. XPS survey for an oxidized and a reduced composite and thin film electrodes.

XPS Surface Analysis of the Composite Electrodes. To observe the change in oxidation state of manganese when the electrode is cycled between 0 and 0.9 V and if ionic species are involved in the charge storage mechanism, the composite electrodes were characterized by X-ray photoelectron spectroscopy (XPS). Prior to the XPS measurements, the composite electrodes were polarized at 0 or 0.9 V until the charge passed was equal to the charge integrated from the cyclic voltammogram. The survey spectra presented in Figure 2 for oxidized and reduced MnO_2-based composite electrodes show Mn 2p (642 eV), Mn 3s (84 eV), and O 1s (530 eV) peaks attributed to manganese dioxide. The C 1s (285 and 293 eV) peaks and F 1s (685 eV) are associated with the presence of acetylene black, graphite, and PTFE. The two spectra are almost identical with the exception of the Na 1s peak that is almost absent for the oxidized composite electrodes (vide infra).

The Mn 3s, Mn 2p, and O 1s core level spectra can be used to assess the change in oxidation state of manganese for the oxidized and reduced MnO_2 electrodes (see Experimental Section). The Mn 3s core level spectra should usually show a peak splitting and a doublet due to the parallel spin coupling of the 3s electron with the 3d electron during the photoelectron ejection.[30,33,34] The energy separation between the two peaks is related to the mean manganese oxidation state. Since a lower valence implies more electrons in the 3d orbital, more interaction can occur upon photoelectron ejection. Consequently, the energy separation between the two components of the Mn 3s multiplet will increase.[30] The inverse trend will be observed when the manganese valency increases.

The Mn 3s core level spectra were recorded (Figure SI5) for oxidized and reduced MnO_2-based composite electrodes, and the relevant data are included in Table 1. The data of Table 1 revealed that the peak splitting of the doublet of the Mn 3s core level spectra is almost

(30) Chigane, M.; Ishikawa, M. *J. Electrochem. Soc.* **2000**, *147*, 2246.
(31) Chigane, M.; Ishikawa, M.; Izaki, M. *J. Electrochem. Soc.* **2001**, *148*, D96.
(32) Long, J. W.; Young, A. L.; Rolison D. R. *J. Electrochem. Soc.* **2003**, *150*, A1161.
(33) Moulder, J. F.; Strickle, W. F., Sobol, P. E.; Bomben, K. D. *Handbook of X-ray Photoelectron Spectroscopy*; Perkin-Elmer Corporation: Physical Electronics Division: Eden Prairie, MN, 1992.
(34) Briggs, D.; Seah, M. P. *Practical Surface Analysis*, 2nd ed,; John Wiley & Sons: 1996; Volume 1.

Table 1. Data Obtained from the XPS Spectra

thin film	Mn 3s (eV)				Mn 2p (eV)		oxidation state Mn 3s/O 1s [b]	O 1s (eV)[c]		
	E (V)	peak 1	peak 2	Δ eV[d]	3/2	ΔBE_{Mn-O}[a]			BE (eV)	area %
oxidized	0.90	88.88	84.10	4.78	642.6	112.8	4.0/4.0	Mn−O−Mn	529.8	80.6
								Mn−OH	531.3	2.9
								H−O−H	532.4	16.5
as-prepared		88.72	83.80	4.92	642.4	112.7	3.6/3.7	Mn−O−Mn	529.7	64.8
								Mn−OH	531.0	20.7
								H−O−H	532.4	14.5
reduced	0	88.98	83.65	5.33	642.3	112.4	2.9/3.1	Mn−O−Mn	529.9	48.6
								Mn−OH	531.1	43.4
								H−O−H	532.6	8.0

composite electrode	Mn 3s (eV)				Mn 2p (eV)		oxidation state Mn 3s/O 1s [b]	O 1s (eV)[c]		
	E (V)	peak 1	peak 2	Δ eV[d]	3/2	ΔBE_{Mn-O}[a]			BE (eV)	area %
oxidized	1.25	88.74	83.65	5.09	642.4	112.7	3.5/3.5	Mn−O−Mn	530.2	50.0
								Mn−OH	531.0	24.9
								H−O−H	533.5	8.5
								SO_4^{2-}	532.0	16.7
	0.9	89.39	84.41	4.98	643.1	112.7	3.5/3.5	Mn−O−Mn	530.3	53.2
								Mn−OH	531.0	26.9
								H−O−H	533.3	9.8
								SO_4^{2-}	532.0	10.1
reduced	0	88.58	83.60	4.98	643.0	112.7	3.5/3.5	Mn−O−Mn	530.3	60.3
								Mn−OH	531.6	30.4
								H−O−H	533.8	6.5
								SO_4^{2-}	532.0	2.8
	−0.65	89.41	84.39	5.02	643.1	112.7	3.5/3.5	Mn−O−Mn	530.2	49.9
								Mn−OH	531.0	25.3
								H−O−H	533.4	8.6
								SO_4^{2-}	532.0	16.2

[a] Difference in binding energy between the Mn $2p_{3/2}$ and O 1s [Mn−O−Mn] peaks. [b] The first entry is obtained by the Mn 3s peak shift and the second after the slash by the relative area calculation of the O 1s components. [c] For the composite electrode, the presence of sulfate was shown by a S 2p peak at 168.6 eV).[33] Hence, a component at 532 eV was added to fit the O 1s peak envelope in order to take into account the contribution oxygen atoms of the sulfate species when computing the Mn redox state. [d] Difference between the binding energies of peak 1 and peak 2.

the same for all the electrodes. This value close to 5.00 eV is compared to 5.79, 5.50, 5.41, and 4.78 eV for reference sample of MnO, Mn_3O_4, Mn_2O_3, and MnO_2, respectively.[30] Hence, the manganese oxidation state remained at about 3.5. Similar findings were obtained for composite electrodes polarized at more positive (1.25 V) and more negative (−0.65 V) potential. The absence of a change of the manganese oxidation state is puzzling in light of previous reports on electrodeposited MnO_2[30,31] and birnessite MnO_x ambigel films[32] in aqueous electrolytes. Even when the XPS measurements were performed with a takeoff angle of 30° or 45°, in conditions where a thinner surface layer is probed,[33,34] attempts to observe a change of the manganese oxidation state failed. Then, it was suspected that the oxidation state of the electrode changed during the drying step and exposure to air. The measurement of the open circuit potential (OCP) for both reduced or oxidized electrodes, monitored before and after the drying step, revealed a drift of the OCP to an average potential of 0.45 V following the drying step. This observation suggests that only the surface MnO_2 may be involved in the redox pseudocapacitive reaction. In this case, the surface of the film could be brought back very close to the oxidation state of OCP conditions by a redox reaction driven by the chemical potential between the surface and the bulk of the material.

Electrochemical Behavior of the MnO_2 Thin Film Electrode. To avoid this phenomenon, thin film electrodes were used to ensure that a more significant fraction of the MnO_2 film would be involved in the electrochemical reaction during the oxidation and reduction steps. This was accomplished by using MnO_2 thin film supported on platinum electrodes as described in the Experimental Section. First, experiments were performed with electrodes of different film thickness to estimate the electrochemically active fraction of the MnO_2 film. The mass and thickness were controlled by adding between one and five drops of a MnO_2−PVdF−HFP mixture with a drying step between each addition (see Table 2). Figure 1B shows a representative cyclic voltammogram for the MnO_2 powder supported on platinum foil, which displays the characteristic capacitive behavior between 0 and 0.9 V. The specific capacitance of 1380 F/g obtained for this electrode is close to the theoretical value of 1370 F/g expected for a redox process involving one electron per manganese atom. The larger polarization of the Pt−MnO_2 electrode relative to the composite electrode (Figure 1A), demonstrated by the more pronounced curvature of the cyclic voltammogram near the potential limits, is due to the absence of the conductive carbon in the thin film electrode. Table 2 shows the variation of the voltammetric charge measured for each electrode as a function of the MnO_2 mass. For the thinner film (electrode A), all the MnO_2 material is taking part in the electrochemical redox process, during the cyclic voltammetry experiment performed at 5 mV/s, since the Coulombic efficiency is about 100%. The Coulombic efficiency is calculated from the measured voltammetric charge of the cyclic voltammogram and the theoretical calculated charge by assuming the transfer of one electron per Mn atom and that the whole MnO_2 mass is electrochemically active. Table 2 indicates that the Coulombic

Table 2. Electrochemical and Composition Data for MnO_2 Thin Film Electrodes with Different Loadings

electrode	mass (μg)	amount of MnO_2 (moles)	voltammetric charge[a] (C)/(C/g)	calculated charge (C)[b]	coulombic efficiency (%)[c]	specific capacitance (F/g)
A	5.0 ± 0.3	5.75×10^{-8}	0.0056/1250	0.0055	101	1380
B	10.0 ± 0.8	1.15×10^{-7}	0.0106/1190	0.0111	95	1320
C	15.0 ± 1.5	1.73×10^{-7}	0.0148/1100	0.0166	89	1230
D	20.0 ± 2.5	2.30×10^{-7}	0.0156/875	0.0222	70	970
E	25.0 ± 3.8	2.88×10^{-7}	0.0186/835	0.0277	67	930

[a] Calculated by taking into account the mass of MnO_2 in the sample (about 89.1%). The first value is in C, whereas the second is the specific voltammetric charge in C/g. [b] The calculated charge was obtained from the amount of MnO_2 on the electrode by assuming the transfer of one electron per Mn atom. [c] Coulombic efficiency (%) = (voltammetric charge/calculated charge) × 100.

efficiency decreased when the film thickness increased and that it reached only 67% for 25 μg of MnO_2. These results demonstrate clearly that a significant fraction of MnO_2 was not electrochemically addressable when the film thickness increased. In contrast, in the case of a rapid protonic diffusion in the bulk of the active material, the charge would increase linearly with the mass of the electrode.[17] This suggests that slower ionic transport is occurring within the active material or that protons cannot diffuse freely across the thickness of the MnO_2 particles (vide infra). This is supported by the relatively low diffusion coefficient (6×10^{-10} cm^2/s) for protons in manganese dioxide.[35]

Some insight into the decrease of the Coulombic efficiency with an increase of the film thickness could be obtained by calculating the surface of the platinum current collector covered by MnO_2 particules. By considering spherical particles with a mean diameter of 420 nm, the formation of a "monolayer" of these MnO_2 particles will require 33 μg. However, as depicted in Figure SI4b, the MnO_2 particles tend to agglomerate rather than forming a monolayer. The MnO_2 deposited on the platinum substrate leads to a larger number of clusters, which reduce the area of material exposed to the electrolyte. If the electrochemical process is taking place only at the surface of the MnO_2 exposed to the electrolyte, the charge will decrease as the weight of MnO_2 is increased. This can explain why thin films usually exhibit higher capacitance values than bulk composite electrodes.[17] In this study, the gravimetric charge of our composite electrodes (100 μm thick) is limited to 135 C/g. On the other hand, when the weight of MnO_2 is much lower as for the Pt−MnO_2 samples, the charge increased up to 1250 C/g for very small amount of MnO_2. This Coulombic efficiency, close to 100%, implies that protons or alkali cations can diffuse through a "monolayer" of MnO_2 particles. This is expected by considering the particle size (<420 nm as can be seen in Figure SI3), the charge/discharge time (180 s for a scan rate of 5 mV/s), and the diffusion coefficient for protons in manganese dioxide.[35] When a larger amount is MnO_2 or when a thicker film is used, the diffusion of active cations is clearly hindered.

XPS Surface Analysis of the MnO_2 Thin Film Electrodes. The survey spectra for the oxidized and reduced thin film electrodes are depicted in Figure 2. These spectra differ slightly from those recorded for the corresponding composite electrode (also shown in Figure 2). These differences become more evident on the higher resolution spectra as it will be demonstrated below.

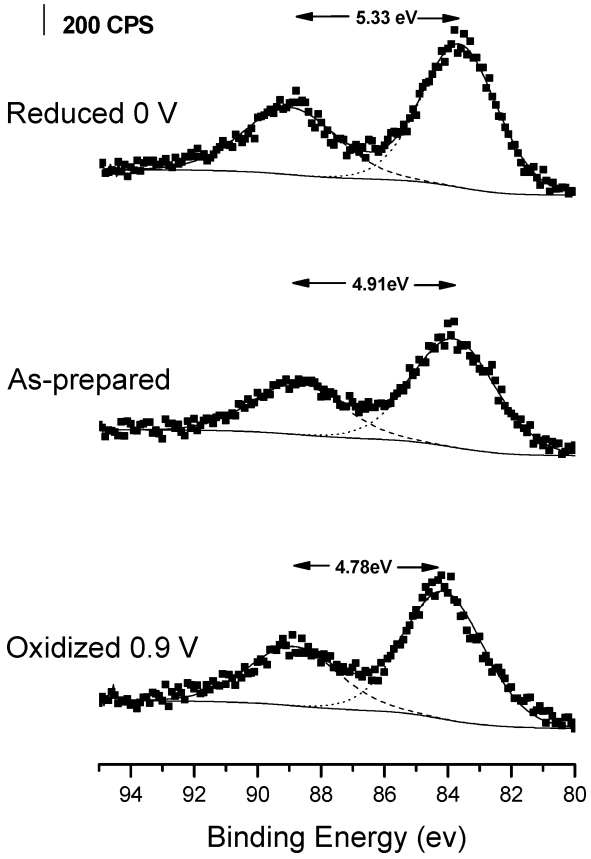

Figure 3. Mn 3s core level spectra for reduced, as-prepared, and oxidized thin film electrodes. The peak separation between the two peaks is indicated and can be used to determine the oxidation state of manganese. The raw data are represented by the dots, and the fitted data are represented by the lines.

Figure 3 depicts the Mn 3s core level spectra for the reduced, as-prepared, and oxidized MnO_2 thin film electrodes. The separation of peak energies (ΔE_b) of the Mn 3s components increased from 4.78 eV for the oxidized film to 5.33 eV for the reduced film (see also Table 1). In the case of the as-prepared thin film, an intermediate value of 4.91 eV was found. The E_b values are in agreement with those expected for Mn^{4+} and Mn^{3+} oxides, which should have a peak separation of about 4.7 and 5.4 eV, respectively.[30,36] In addition, it was previously shown that a linear relation exists between the energy separation of the Mn 3s peaks and the oxidation state of manganese in the oxide.[21,30,31] From this relationship, the mean manganese oxidation state can be established at 4.0, 2.9, and 3.6 for the

(35) Ruetschi, P. *J. Electrochem. Soc.* **1984**, *131*, 2737.

(36) Audi, A. A.; Sherwood, M. A. *Surf. Interface Anal.* **2002**, *33*, 274.

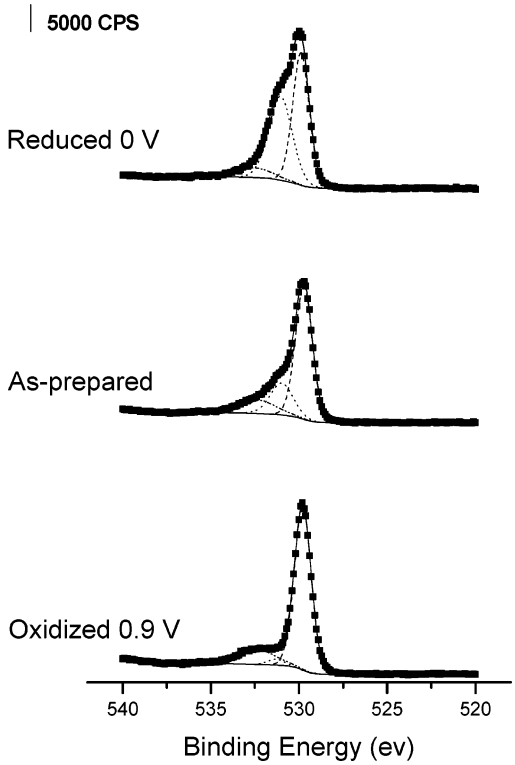

Figure 4. O 1s core level spectra for reduced, as-prepared, and oxidized thin film electrodes. The raw data are represented by the dots, and the fitted data are represented by the lines.

oxidized, reduced, and as-prepared electrodes, respectively. Thus, in contrast to the thicker composite electrode, a change of the oxidation state of manganese can be observed for the thinner film electrode on platinum substrate. This change is also accompanied by a color change upon redox switching.

The O 1s core level spectra were also used to confirm the change of manganese oxidation state during redox switching. Figure 4 shows a significant difference of the O 1s envelope between the reduced, as-prepared, and oxidized thin film electrodes. Indeed, the reduced film shows a distinct high-intensity shoulder on the higher binding side of the main peak. To get some insight into the chemical modification that are occurring upon redox switching, the O 1s spectra were analyzed by curve fitting. Figure 4 (see also Table 1) shows that the spectra can be fitted with three components which are related to the Mn−O−Mn bond (529.8 ± 0.1 eV) for the tetravalent oxide, the Mn−OH bond (531.1 ± 0.2 eV) for an hydrated trivalent oxide, and finally to a H−O−H bond (532.5 ± 0.1 eV) for residual structure water.[28,37,38] So, the change of the shape of the O 1s envelope is caused by the variation of the Mn−O−Mn and Mn−OH contributions (Table 1). For the oxidized electrode, the Mn−O−Mn component contributes to about 81% of the O 1s peak, whereas for the reduced electrode, the intensity of the Mn−O−Mn and Mn−OH signals is almost identical. The variation of the relative intensity of the O1s components indicates a change of the manganese oxide oxidation state between the oxidized and reduced states. Table 1 indicates that the mean manganese oxidation state, obtained from eq 5, is equal to 4 for the oxidized electrode, whereas, for the reduced electrode, an oxidation level of 3.1 is found. In the case of the as-prepared electrode, an intermediate oxidation state of 3.7 is determined. These values are in excellent agreement with those computed from the Mn 3s data (vide supra).

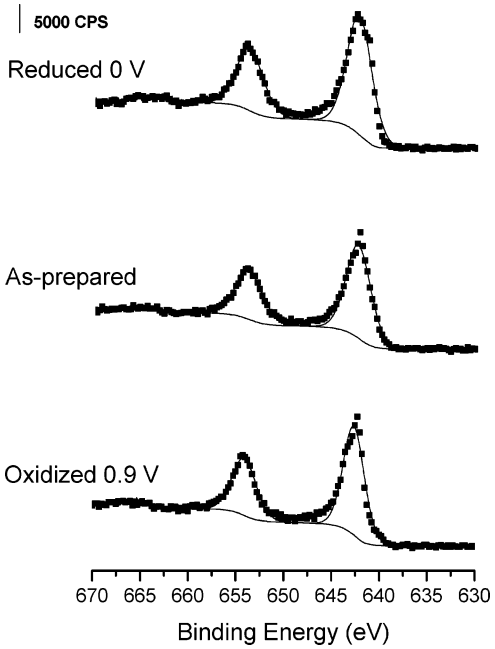

Figure 5. Mn 2p core level spectra for reduced, as-prepared and oxidized thin film electrodes. The raw data are represented by the dots, and the fitted data are represented by the lines.

Figure 5 shows Mn 2p spectra of thin film samples. Such Mn 2p core level spectra have been recently used to determine the contribution of various Mn species.[28] However, the evaluation of the Mn(II), Mn(III), and Mn(IV) contributions rely on a curve fitting procedure, which can be arbitrary since the shape of the spectra of the electrodes does not appear to change drastically (Figure 5). Nevertheless, the binding energy separation (ΔE_{Mn-O}) between the Mn $2p_{3/2}$ and O 1s [Mn−O−Mn] peaks has been found to change slightly when the electrode is oxidized or reduced.[30,33] As shown in Table 1, the ΔE_{Mn-O} values were found to be equal to 112.4 and 112.8 eV for the reduced and oxidized film electrodes, respectively. The larger ΔE_{Mn-O} for the oxidized thin film is in agreement with literature data[31] despite the fact that the absolute reported value was slightly larger. Thus, all the XPS data are consistent with a change of manganese oxidation state upon switching between 0 and 0.9 V. The redox switching of MnO_2 electrodes might involve ionic species from the electrolyte solution (0.1 M Na_2SO_4), and the appropriate XPS core level spectra (Na 1s and S 2p) were measured to further characterize the charge storage mechanism.

Figure 6 shows that the intensity of the Na 1s peak is larger for the reduced thin film (thin film, 0 V) in comparison to the oxidized electrode (thin film, 0.9 V). This is consistent with a charge compensation of MnO^- by Na^+ for the reduced film (eq 3). In addition, Figure 6 demonstrates that the sulfate anions are not involved in the redox process, since the S 2p spectra are featureless. This is to be contrasted with the significant

(37) Banerjee, D.; Nesbitt, H. W. *Geochim. Cosmochim. Acta* **1999**, *63*, 3025.
(38) Banerjee, D.; Nesbitt, H. W. *Geochim. Cosmochim. Acta* **2001**, *65*, 1703.

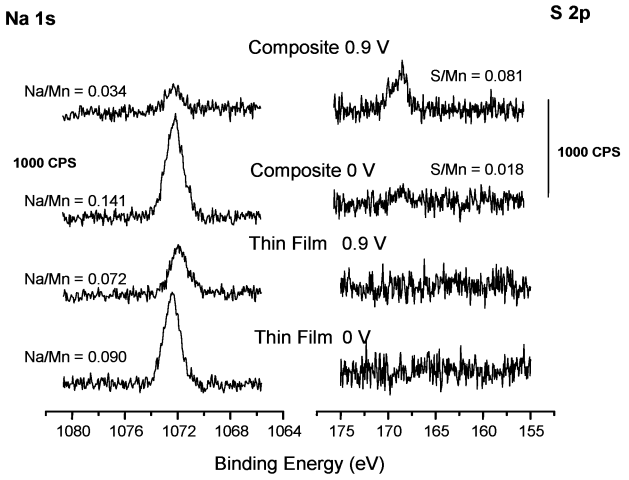

Figure 6. Na 1s and S 2p core level spectra for composite and thin film electrodes.

difference in the variation of the Na 1s and S 2p spectra for the composite electrode. When the composite electrode is switched from 0 to 0.9 V, the Na 1s signal decreased, whereas the S 2p signal increased. Obviously, some salt seems to be trapped since both Na^+ and SO_4^{2-} are found in the electrodes. The oxidized composite electrode contains an excess of sulfate (ratio S/Mn = 0.064), whereas the reduced electrode has an excess of Na^+ (ratio Na/Mn = 0.105). The variation of the Na^+ and SO_4^{2-} concentrations for the composite electrode may appear puzzling considering that the valence of manganese does not appear to change between the oxidized and reduced states. The excess of Na^+ and SO_4^{2-} for the reduced and oxidized electrodes, respectively, can be attributed to the presence of carbon in the composite electrodes. Thus, this behavior is consistent with that expected for a classical double layer charge storage process.[1] The invariance of the manganese oxidation state for the composite electrodes which contrasts with the change observed for the thin film electrodes suggests that only a thin layer of MnO_2 on the electrode is involved in the redox interconversion. This is also confirmed by the high capacitance recorded for the thinner films, which almost reached the theoretical values (vide supra).

The variation of the Na/Mn ratio, for the thin film electrode, upon potential switching deserves some comments. As mentioned above, the higher Na/Mn ratio for the reduced electrode in comparison to the oxidized electrode is consistent with a charge compensation of $MnOO^-$ by Na^+. On the other hand, the Na/Mn is much lower than that expected for a complete compensation by Na^+. These results clearly demonstrate that protons are involved in the redox process of MnO_2. Despite these experimental XPS results, the exact mechanism for the uptake of Na^+ is unclear. Recent electrochemical measurements of the intercalation of alkali metal ions into birnessite manganese dioxide in aqueous media suggested that protons are directly intercalated but not the alkali metal cations.[39] The presence of the alkali metal cations in the oxide matrix was explained by an ion-exchange reaction between the cations and H^+. Accordingly, a similar mechanism cannot be ruled out completely for our electrodes.

Conclusion

In this work, the charge storage mechanism in MnO_2 electrode, used in aqueous electrolyte, was investigated by cyclic voltammetry and X-ray photoelectron spectroscopy. The main objective was to determine whether the manganese oxidation state changed during potential switching between 0 and 0.9 V vs Ag/AgCl. To this end, thin MnO_2 films deposited on a platinum substrate and thicker MnO_2 composite electrodes were used. X-ray photoelectron spectroscopy (XPS) measurements (Mn 3s and O 1s) with the thick composite electrodes did not reveal any change that could be assigned to a variation of the manganese valency, and, at this point, the charge storage mechanism could be based on electrostatic effects only. In fact, the charge storage would be similar to that observed for carbon electrodes.[1] On the other hand, a completely different XPS behavior was noticed for the thin film electrodes. Both the Mn 3s and O 1s spectra were consistent with manganese oxidation states of +3 and +4 for the reduced and oxidized forms, respectively. The XPS data also show that Na^+ cations from the electrolyte are involved in the charge storage process of MnO_2 thin film electrodes. The Na/Mn ratio for the reduced electrode is much lower than what is anticipated for charge compensation dominated by Na^+ and suggests the involvement of protons. The apparent discrepancy between the XPS data (Mn 3s and O 1s spectra) can be explained by the cyclic voltammetry data of the thin film electrodes which established that only a thin layer of MnO_2 is involved in the redox process and is electrochemically active. Presumably, this thin surface layer cannot be probed for the composite electrode because this region is brought back to the chemical (oxidation) state of the bulk by internal redox interconversion.

Acknowledgment. The financial support of the Natural Science and Engineering Research Council (NSERC) and the Canadian Foundation for Innovation (CFI) is acknowledged. One of the authors (T.B.) would like to thank "l'Université de Nantes" for giving him the opportunity to work in UQAM and UQAM for welcoming him as a visiting professor. The "Ministère Français des Affaires Etrangères" and the "Ministère des Relations Internationales du Québec" are also greatly acknowledged for supporting this work within the framework of the "Commission Permanente de Coopération Franco-Québécoise" (project #59-102).

Supporting Information Available: X-ray diffraction pattern of the as-synthesized MnO_2 powder (Figure SI1), scanning electron micrograph of the as-synthesized MnO_2 powder (Figures SI2 and SI3), scanning electron micrographs of a MnO_2 composite electrode (Figure SI4a), scanning electron micrograph of MnO_2 powder−PVdF−HFP coated on Pt (Figure SI4b), and Mn 3s core level spectra (Figure SI5). This material is available free of charge via the Internet at http://pubs.acs.org.

CM049649J

(39) Kanoh, H.; Tang, W.; Makita, Y.; Ooi, K. *Langmuir* **1997**, *13*, 6845.